Paleomagnetism Conglomerate Test on Archean Conglomerate Rock from Jack Hills, Australia

by

Rachel Bowens-Rubin

Submitted to the Department of Earth, Atmospheric, and Planetary Science
in partial fulfillment of the requirements for the degree of

Bachelor of Science in Earth, Atmospheric, and Planetary Science

at the

MASSACHUSETTS INSTITUTE OF TECHNOLOGY

June 2011

Author ... Signature redacted .....
Department of Earth, Atmospheric, and Planetary Science
May 16, 2011

Certified by..... Signature redacted .....
Benjamin Weiss
Professor, Departments of EAPS
Thesis Supervisor

Accepted by ... Signature redacted .....
Samuel Bowring
Chair, Committee on Undergraduate Program

Paleomagnetism Conglomerate Test on Archean Conglomerate Rock from Jack Hills, Australia

by

Rachel Bowens-Rubin

Submitted to the Department of Earth, Atmospheric, and Planetary Science
on May 16, 2011, in partial fulfillment of the
requirements for the degree of
Bachelor of Science in Earth, Atmospheric, and Planetary Science

Abstract

A paleomagnetism study known as a conglomerate test was run on an Archean sandstone conglomerate rock to determine if the sample contained a remnant magnetization from the time of its formation. Twenty-nine clasts from a thin section of the sample were thermally demagnetized up to a temperature of 395°C. The heating revealed two components of magnetization which were unblocked at low and mid temperatures, revealing a magnetic mineralogy of Pyrrhotite.Eight matrix samples were heated to a temperature of 650°C which revealed two components of magnetization at mid and high temperatures, providing evidence for a magnetic mineralogy of Hematite.The direction of measured magnetic moment of the clasts were statistically similar, indicating that the rock failed the conglomerate test and was remagnetized after the rock formed.

Thesis Supervisor: Benjamin Weiss
Title: Professor, Departments of EAPS

Acknowledgments

I would like to acknowledge everyone in the Paleomagnetism Lab at MIT with extra special thanks to my advisor Ben Weiss, Eduardo Lima, Kyle Bradley, Sonia Tikoo and Jennifer Buz. I would also like to thank Jane Connor, Katie Decker French, and Elizabeth George for their help writing and fighting with LaTeX. And last but not least, Danbee Kim, David Keazer, and Stephen Schwartz for their late night support.

Contents

List of Figures

List of Tables

Chapter 1

Introduction

1.1 Introduction

Over the period of the formation of the Earth, the Earth acquired a magnetic field. The exact time that Earth's magnetic field appeared has been constrained by studying of the natural remnant magnetization (NRM) in ancient Earth rocks. The best age estimate from a recent paleomagnetism study estimates that the Earth gained its magnetic field prior to 3.42 $\pm$ 0.03 billion years ago. (Tarduno, 2010) No studies have been published measuring the remnant magnetization in a sample magnetically imprinted in the Hadean Era (4.6 to 3.8 billion years ago). The aim of this thesis was to measure a conglomerate rock which formed in the Archean era, that contained material from the Hadean Era, in hopes that it may hold the oldest discovered record of the Earth's magnetic field.

1.2 Paleomagnetism

Paleomagnetism is the study of the magnetic recording properties of rocks (Tauxe 2010). By understanding a rock's magnetic properties, records can be extracted about the Earth and other planetary bodies where these rocks resided.

1.2.1 Acquiring Remnant Magnetization

To understand how rocks acquire a magnetic moment, the properties of electrons in ensembles must be considered. Electrons have charge and angular momentum which gives them their own magnetic dipole moment. The direction of this dipole moment depends on the direction of their angular momentum. When the dipole moments of an ensemble of electrons are oriented in the same direction, a stronger net moment is produced. In nonmagnetic materials this alignment does not occur because electrons are paired with other electrons which have angular momentum in the opposite direction. In materials with magnetic imprints, some electrons are left unpaired.

Unpaired electrons like to align their magnetic dipole moment to external magnetic fields. Because of the energy associated with quantum interactions between the electrons (such as the Pauli Exclusion Principle and Hund's Rule), the unpaired, aligned electrons stay in the same direction when the external field is removed. This causes a "Remnant Magnetization" to be left in the material (Tauxe 2010).

Demagnetization of the material occurs when another type of energy dominates over the energy associated with the aforementioned quantum effects (called the exchange energy). One type of energy which can cause the unpaired, aligned electrons to change direction is thermal energy. The temperature at which the thermal energy dominates the exchange energy is known as the "Currie Temperature" in ferromagnetic materials and the "Néel Temperature" in paramagnetic materials (Butler 1992).

1.2.2 Conglomerate Test

A "conglomerate test" is an experiment used in paleomagnetism to determine the relative age of a conglomerate rock's formation to the age of the imprint of its magnetization. The order of these ages can be determined by measuring the direction of the characteristic magnetization in the clasts (Figure 1-1). After overprinting is removed by heating the samples (thermal demagnetization), if the clasts are pointing in random directions, the magnetization was acquired before the formation of the con-

glomerate. If they are pointing in the same direction, the rock has been remagnetized since its formation.

For a clast to preserve an ancient magnetic field, it must have remained unaltered by metamorphic events. Any metamorphic event affecting the rock must have occurred at a lower temperature than the blocking temperature of the magnetic mineral. For this reason, the mineral carrying the magnetic moment must have a high blocking temperature and a single domain grain structure. This mineral must also have remained unaltered chemically through any metamorphic events (no new magnetic materials could have formed during the metamorphism) (Usui 2009).

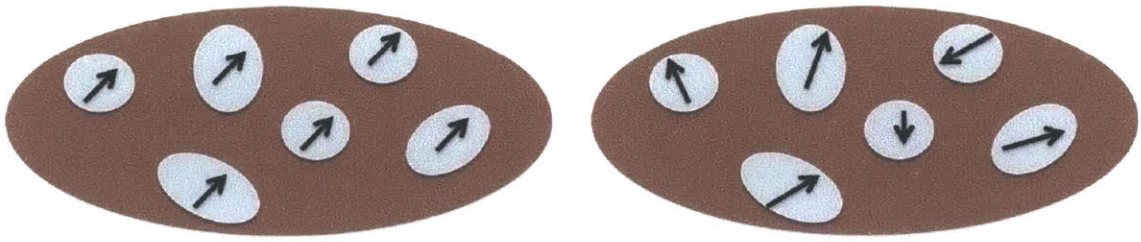

Figure 1-1: Possible Conglomerate Test Results. The white ovals represent the clasts, the black represents the matrix of a conglomerate rock, and the arrows represent the direction of the magnetic moment in the clasts. (Left) If magnetic moment in each of the clasts is pointing in the same direction, the sample was remagnetized after forming into a conglomerate rock. (Right) If the magnetic moment in the clasts point in random directions, the clasts may contain an imprint of the Earth's field from before the time the conglomerate formed.

1.3 Jack Hills

1.3.1 The Importance of the Jack Hills area

The Jack Hills Greenstone Belt is an area located in the southern part of the Narryer Terrane on the Yilgarn Craton in Western Australia. This area is famous because zircons in the surrounding rock have been $^{40}Ar/^{39}Ar$ dated to 4.4 billion years old. The majority of the zircons found in the Jack Hills area were aged at 3.7 billion year ago (Spaggiari, 2007).

1.3.2 EHJH5

The sample studied in this thesis, EHJH5, is a sandstone conglomerate rock from the Narryer Terrane in Australia. EHJH5 was removed in June 2001. It was then transported to the Massachusetts Institute of Technology and stored in the basement of Building 54 until September 2010.

Before EHJH5 was removed from its outcrop position, a mark was made on the sample (black line on Figure 1-2). The right-hand strike and dip of the sample was measured using this mark to be 92° and 96° respectively.

Figure 1-2: EHJH5 before Outcrop Removal. EHJH5 was broken off an outcrop in the Jack Hills Greenstone Belt. A line was drawn on the sample and the right-hand strike and dip was measured relative to this line to be 92° and 96° respectively.

Chapter 2

Methods

2.1 Orientating EHJH5

2.1.1 Overall Orientation Relative to Flat Side

Before cutting occurred, an new orientation system was established relative to the "Flat Side" of EHJH5. (Figure 2-1 indicates which side of EHJH5 is referred to as the "Flat Side.") The right-hand strike and dip of this side were found, and then cutting was performed parallel to this surface.

To find the new dip and right-hand strike of the Flat Side, the original outcrop position of EHJH5 was recreated in the lab. The sample was placed on a base of clay on a table with parallel lines. The parallel lines were designated East/West and the sample was adjusted on its clay base to match the field strike and dip relative to the lines on the table. A protractor was used to perform the alignment with the field orientation. Figure 2-2 shows the alignment of the field dip.

Once EHJH5 was in position, the right hand strike and dip of the flat side were measured. The strike of the flat side was measured to be 186±1° and the dip was measured to be 91±1°. A grid was then drawn on the flat side in the directions of the new strike and up/down. Arrows were also added pointing in the direction of the right-hand strike (Figure 2-3).

After marking orientation lines on the sample, a sheet of 0.5-inch thick acrylic was

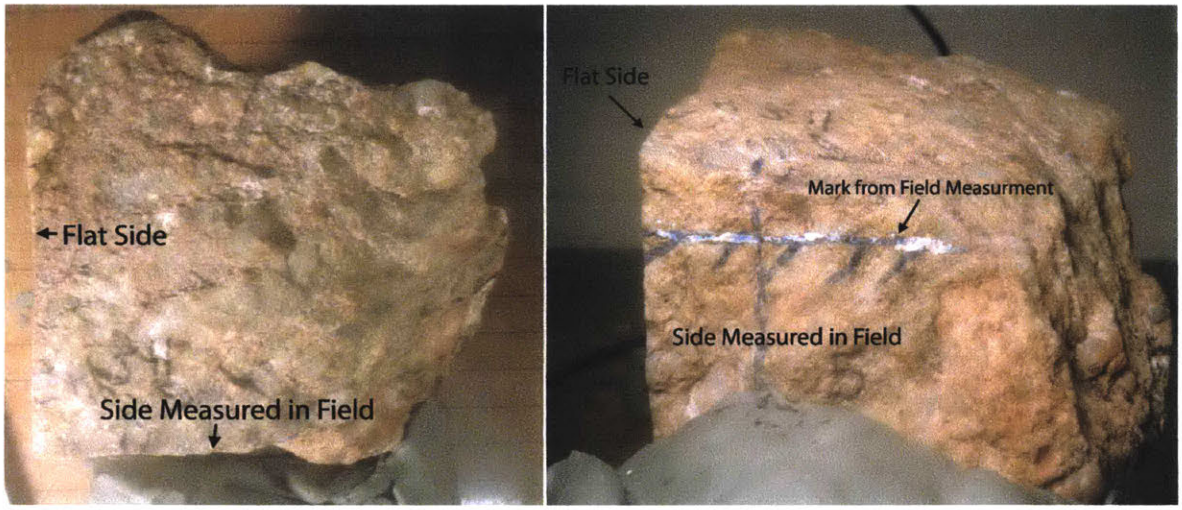

Figure 2-1: Transforming Orientation Systems. An orientation system was established relative to the "Flat Side" of EHJH5 instead of the direction measured in the field. (Left) Top view of EHJH5 (Right) Side view of the side of EHJH5 measured in the field. The mark used to measure the strike and dip in the field is visible.

glued to the flat side using nonmagnetic cyanoacrylate cement. The acrylic provided protection against crumbling as well as a good clamping surface to place the sample on the saw.

2.1.2 Maintaining Orientation when Cutting

As EHJH5 was cut, the grid lines were transferred to each newly cut slab on the side opposite the flat side (which this thesis refers to as the "Harvard" side). *Arrows on the "Harvard" Side of the sample were drawn mirror imaging the flat side (against normal convention which points in the right hand strike direction).* These left handed strike arrows are seen on the samples measured in the magnetometer (Figure 2-4). Although the arrows were drawn in the direction of the left handed strike, all values of the strike mentioned in this thesis are reported in the right hand direction.

Grid lines and other symbols were added so every clast being targeted for extraction would have at least one orientation line. Dots were added to the grid lines to distinguish the up/down lines. These dots were added in a different color to avoid the dots being mistaken for arrows. Figure 2-4 shows an example of a clast that dots

Figure 2-2: Recreating Original Outcrop Dip. EHJH5 was realigned with the original dip and strike measured in the field. A protractor was used to measure this original dip (96°). The blue parallel lines on the rock face are represent the up/down direction in true outcrop coordinates.

and arrows which were drawn to help maintain orientation.

In preparation for high temperature thermal demagnetization, the orientation lines were painted on the samples with white out. This allowed the orientation of the clasts to be maintained above temperatures in which ink from permeant marker evaporates. The number-letter designation was also painted onto each samples in white out.

The dip and right-hand strike of the Harvard side of the slab were 89° and 6° respectively (found from the measurement of the strike and dip of the flat side). Clast and matrix samples' NRMs were later measured using the orientation on the Harvard Side.

Figure 2-3: New Grid System on Flat Side. Lines were drawn on the flat side of EHJH5 after the side's strike and dip were measured. Acrylic was glued on the side shown to help prevent crumbling when the sample was cut.

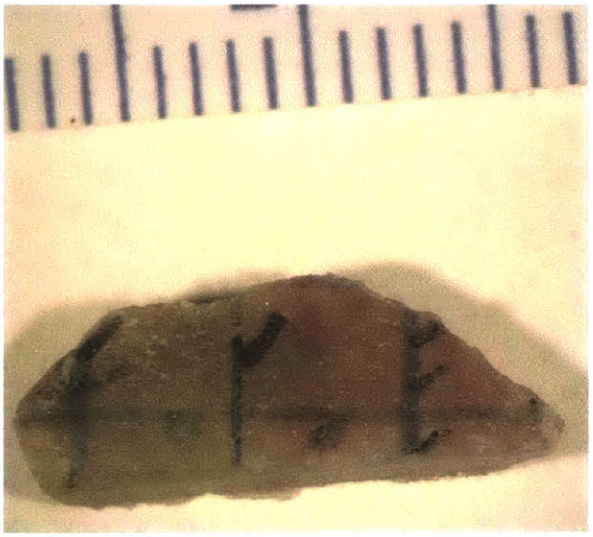

Figure 2-4: Orientation Marking Conventions: Dots and Arrows on Clast 4E. Like sample Ivysaur 4E, each extracted clast contained at least one grid line. Dots and arrows were added to the up/down and strike lines to distinguish between them. The dots were drawn in light green and the arrows were drawn in black.

2.2 Clast extraction

In order to extract clasts from the main body of EHJH5, the sample was gradually broken into smaller parts. The terminology which will be used for the remainder of this thesis to describe the parts from largest to smallest is the following:

1. Slabs (or layers)
2. Sections
3. Pieces
4. Clast/matrix (samples)

2.2.1 Slabs

A water-cooled brick saw, located in Building N9 at MIT, was used to begin the slabbing. Part way through the first cut, the saw become inoperable. Cutting was continued using a oil-cooled brick saw located at Harvard University in the Museum of Natural History Building. The first cut using the oil saw was made approximately 0.5-cm closer to the interior of the sample than the previous cut. The offset between the cuts made at MIT and Harvard created a thin section. This thin section was broken off from the rest of the layer (by hand) and is referred to for the duration of this thesis as the section named Bulbasaur.

Two additional cuts were made using the Harvard saw which were parallel to the flat side of EHJH5. This created three slabs which are referred to as Ivysaur, Charmander, and Squirtle for the duration of this thesis. Each slab was between 0.3-cm and 0.75-cm in thickness. Ivysaur, which also contained the section "Bulbasaur," was closest to the interior of EHJH5, and Squirtle was closest to outside and contained the flat side of EHJH5. (Figure 2-5 shows the Ivysaur/Bulbasaur, Charmander, and Squirtle aligned together.)

2.2.2 Sections

The Ivysaur, Charmander, and Squirtle layers were each divided into three to seven sections. Most sections were separating by breaking the slabs by hand, but some

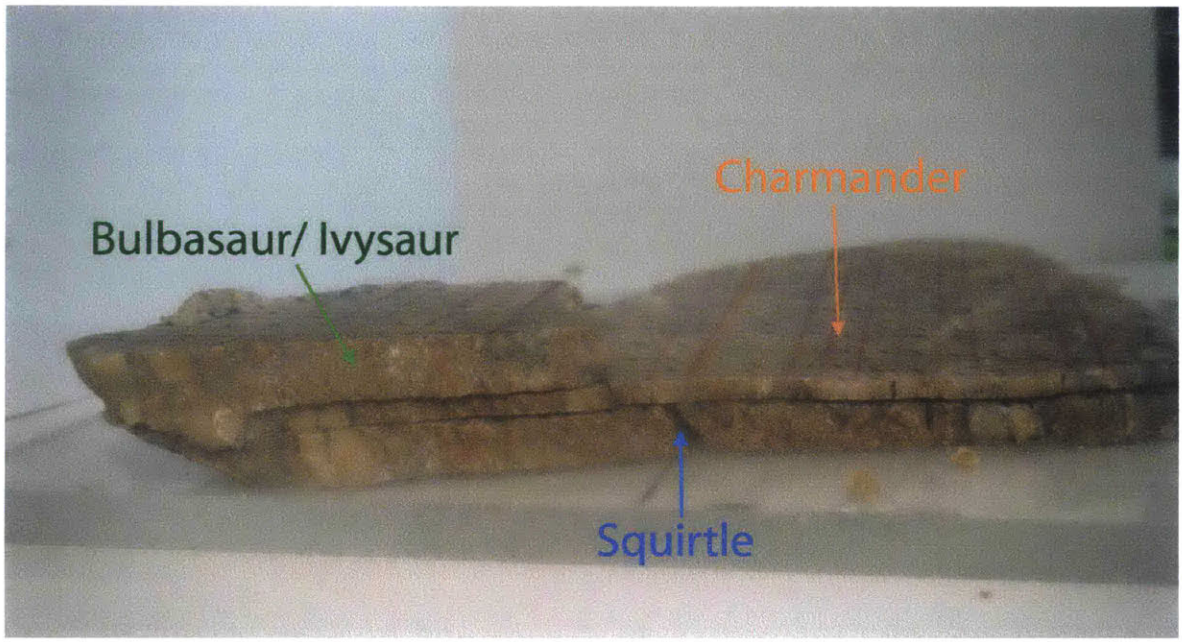

Figure 2-5: Three Layers of Slabs. The Bulbasaur/Ivysaur layer was closest to the interior of EHJH5, Charmander was in the middle, and Squirtle was closest the exterior. Squirtle contained the Flat Side glued to the acrylic, which is facing the table. Only a part of each slab is stacked for this photograph.

needed to be separated by cutting. When cutting was necessary, a diamond precision wire saw was used. This saw was located at MIT in building 54.

The Bulbasaur/Ivysaur layer was divided into seven sections: Bulbasaur, Ivysaur 1 through 5 and Ivysaur 0. Ivysaur 0 represented the pieces which fell off during the slab cutting. Figure 2-6 shows Ivysaur sections 1 through 5 and Figure 2-7 shows Bulbasaur with the rest of the Ivysaur layer.

Charmander was broken into three sections: Charmander 1 and 2 and Charmander 0. Charmander 0 represents the pieces which fell off during the slab cutting. Charmander 1 and 2 have not been divided into pieces. (Figure 2-8)

Squirtle was broken into six sections: Squirtle 1 through 5 and a section which was not removed from the acrylic plate. No Squirtle section has been divided into pieces. (Figure 2-9)

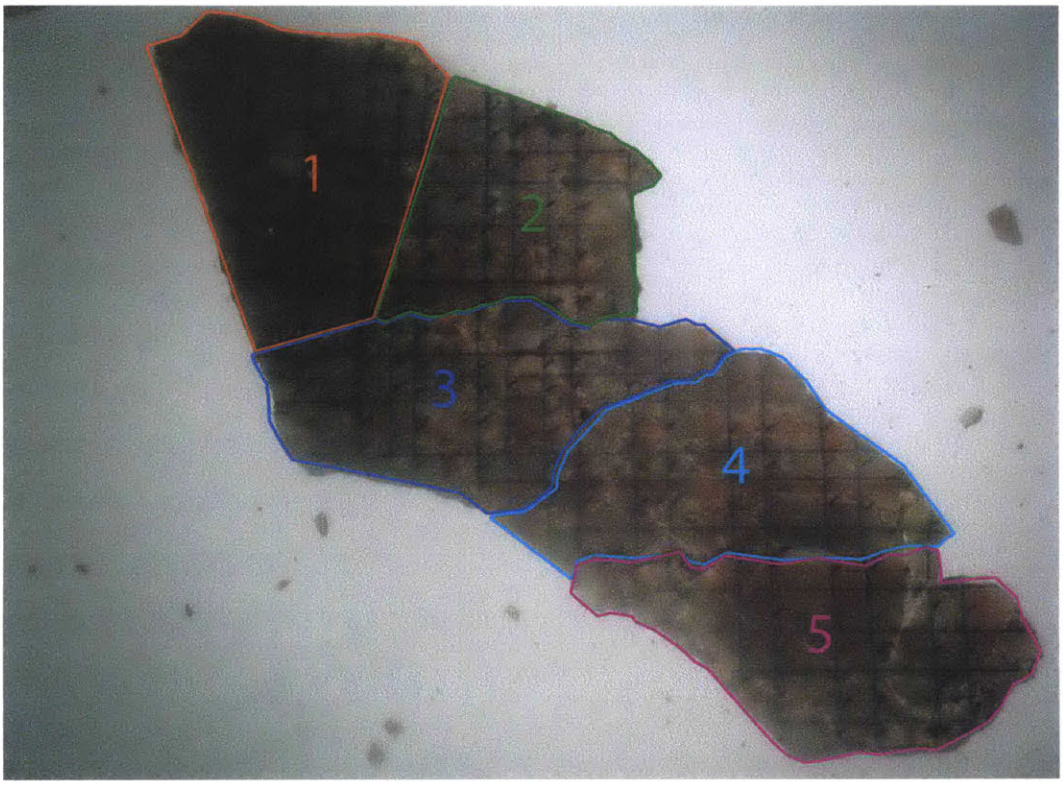

Figure 2-6: Ivysaur Sections. Ivysaur was divided into five sections in addition to pieces which crumbled off during the slab cutting. The crumbled off pieces (referred to as Ivysaur 0) are not shown in this picture.

2.2.3 Pieces and Clast/Matrix

The Ivysaur sections 0 through 5 and Bulbasaur were broken into pieces for clast and matrix extraction. Most pieces were separated using the diamond precision wire saw, located at MIT in building 54, but some were broken apart by hand. Clasts were extracted from the pieces using the same saw. Once extracted, the clasts were sanded to remove any matrix material remaining.

Matrix samples were extracted by the same cutting method as the clasts, and were intensionally selected in pairs across sections in order to check if the sections had been remagnetized since their separation. The following matrix samples were physically near each other: 1F and 2B, 1H and 2Ki, 3G and 2Kii, and 1K and 3A.

Table 2.1 gives a summary of the clast and matrix samples extracted from each section. Figure 2-10 through Figure 2-16 show the pieces and clasts which were cut

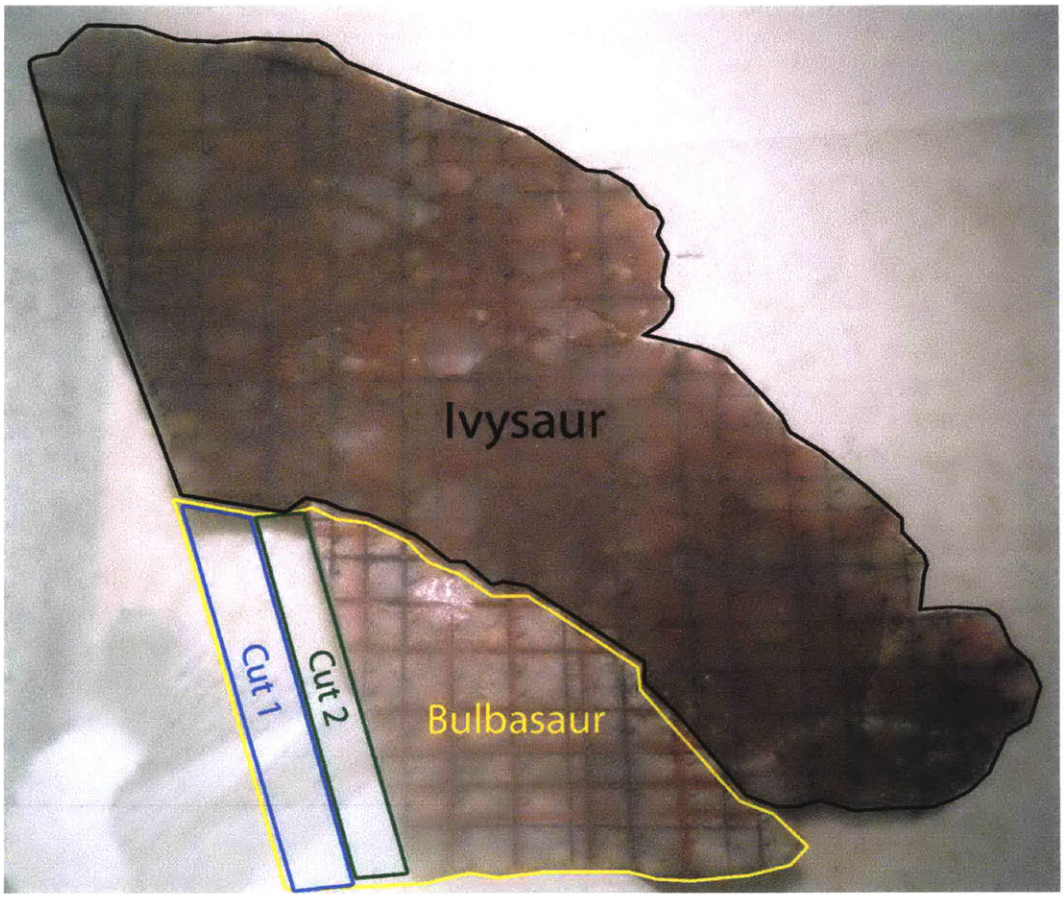

Figure 2-7: Bulbasaur with Ivysaur. The Bulbasaur section, which was broken off during the slab cutting, is in the same layer as the Ivysaur sections. The pieces cut off of Bulbasaur for clast extraction are not photographed but are roughly outlined.

from each section. Three sets of clast samples originated from the same parent clasts: 1F, 1Gi, and 1Gii; 4Mi and 4Mii; and 5Gi and 5Gii.

2.3 Measuring

Magnetic moment measurements were taken using a Superconducting Quantum Interference Device (SQUID) magnetometer at MIT in Building 54. The software *Paleomag* was used to control the magnetometer.

To load a sample into the magnetometer, each sample first needed to be mounted on a quartz disc. Nonmagnetic cyanoacrylate cement (*Instant Krazy glue*) was used to

Figure 2-8: Charmander Sections. Charmander was broken into two sections in addition to pieces which crumbled off during the slab cutting. The crumbled off pieces are shown in yellow and are designated as section *Charmander 0.*

mount the Harvard side of each of the samples to the disc. A line was then drawn on the bottom of the quartz disc which went through the "Up" direction of the sample (Figure 2-17). This line was used to align the sample on a rod which lowered the sample into the measurement region of the SQUID magnetometer.

The magnetic moment of the quartz discs were measured before the samples were mounted. No disc was used which exceeded a magnetic moment of 5×10^{-9}A m^2. A measurement of the magnetic moment of the background was also taken at the start of run of measurements. The background measurement never exceeded 4.5×10^{-9}A m^2.

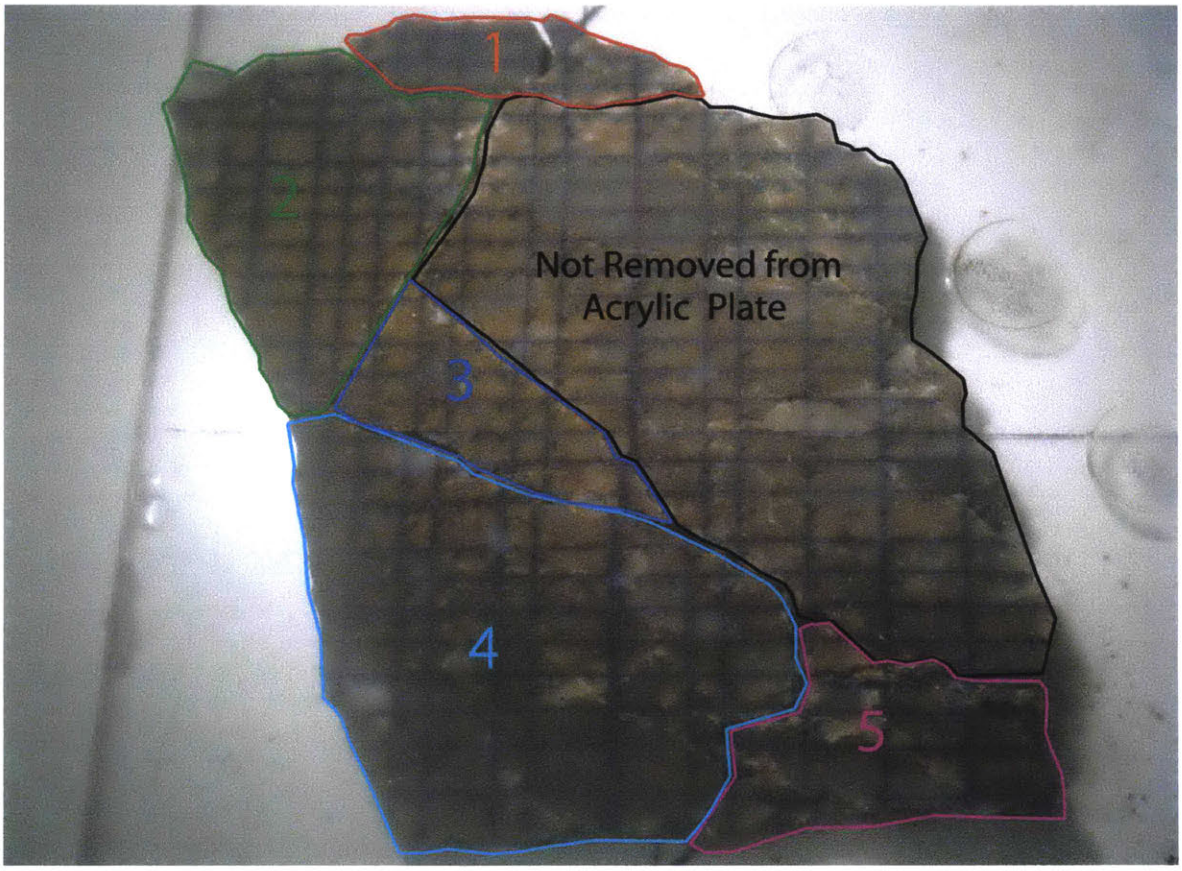

Figure 2-9: Squirtle Sections. Squirtle was divided into 5 sections which were removed from the acrylic plate. Some material was left glued to the acrylic.

During the measurement period, the samples were kept inside a magnetically shielded room (<200nT).

2.4 Heating

To run a thermal demagnetization of the the clasts and matrix samples, the samples were heated in a *Thermal Specimen Demagnetizer* made by ASC Scientific. The samples were loaded into the oven unidirectionally (Figure 2-18). For each temperature step, the direction the samples were loaded was flipped to prevent imprinting from any small magnetic field inside the oven.

Table 2.1: Pieces, Clasts, and Matrix Extracted by Section

Section	# Pieces	# clasts	# matrix	Guide	Samples same Parent Clast
Bulb	17	5	0	Fig. 2-10	1F, 1Gi, and 1Gii
Ivy0	11	5	0	Fig. 2-16	–
Ivy1	11	8	3	Fig. 2-11	–
Ivy2	12	8	2	Fig. 2-12	–
Ivy3	12	9	2	Fig. 2-13	–
Ivy4	12	9	0	Fig. 2-14	4Mi and 4Mii
Ivy5	10	8	0	Fig. 2-15	5Gi and 5Gii

Figure 2-10: Bulbasaur Guide. Bulbasaur was broken into two small parts in order to extract smaller pieces from the slab. The pieces obtained from cut 1are outlined in blue, and the pieces obtained from cut 2 are outlined in green. Clasts were then extracted from pieces 1B, 1F, 1G, and 1K. Clasts 1F, 1Gi and 1Gii originated from the same clast.

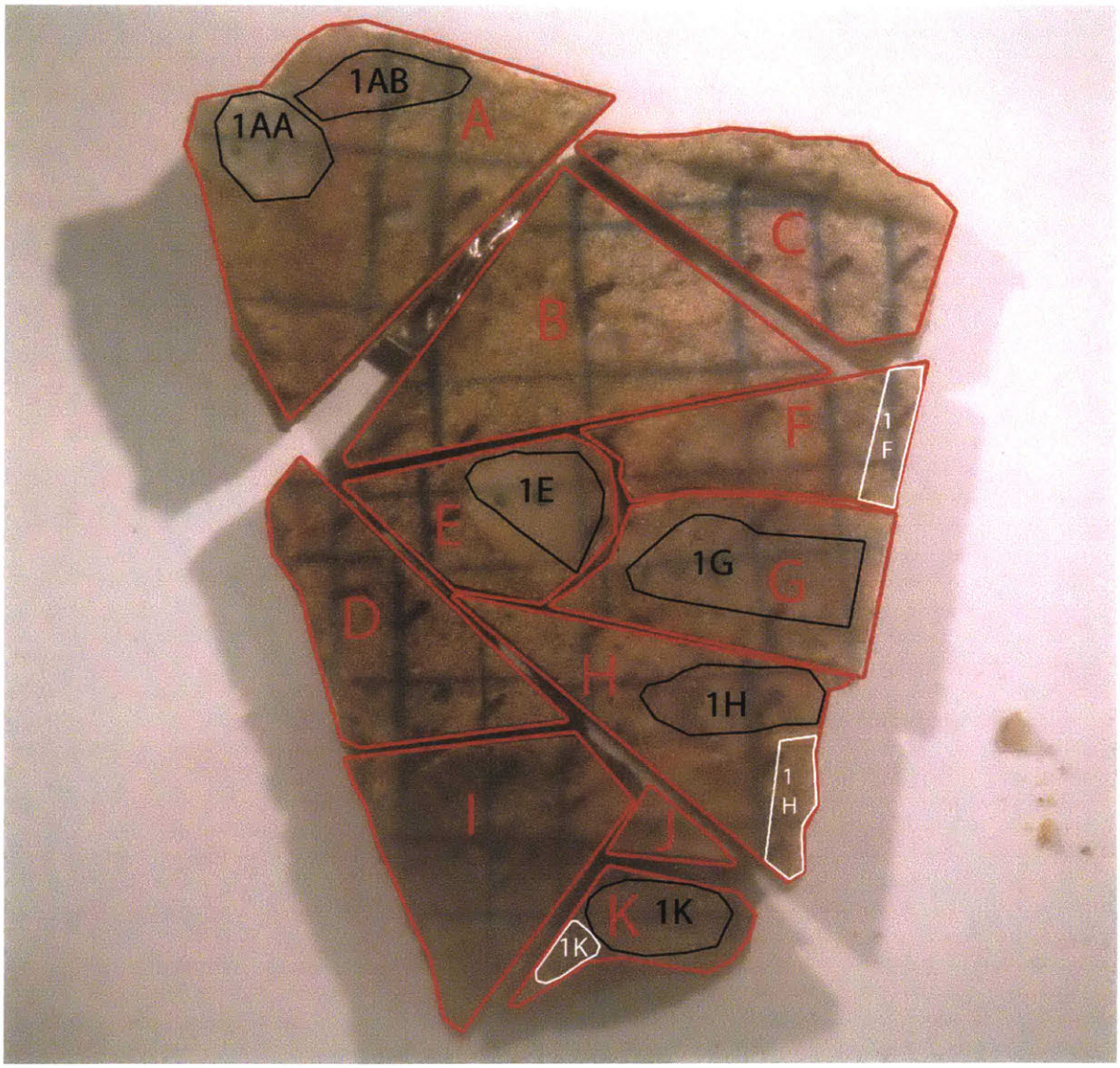

Figure 2-11: Ivysaur Section 1 Guide. Clasts were extracted from 1A, 1E, 1G, 1H, and 1K and are outlined in black. Two clasts were extracted from 1A which were not from the same parent clast. Matrix samples were extracted from 1F, 1H, and 1K and are outlined in white.

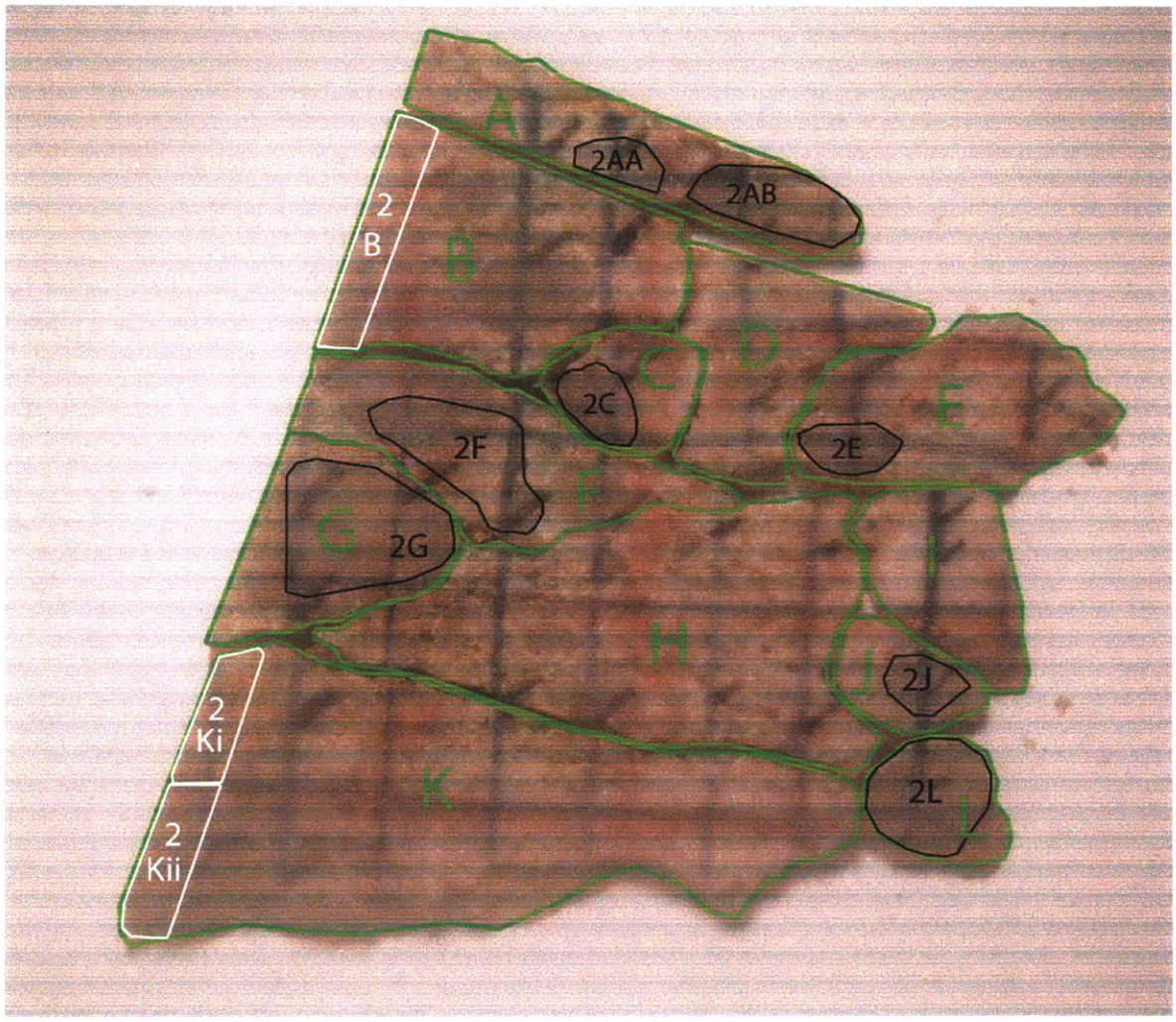

Figure 2-12: Ivysaur Section 2 Guide. Clasts were extracted from 2A, 2C, 2E, 2F. 2G, 2J, 2L and are outlined in black. Two clasts were extracted from 2A which were not from the same parent clast. Matrix samples were extracted from 2B and 2K and are outlined in white.

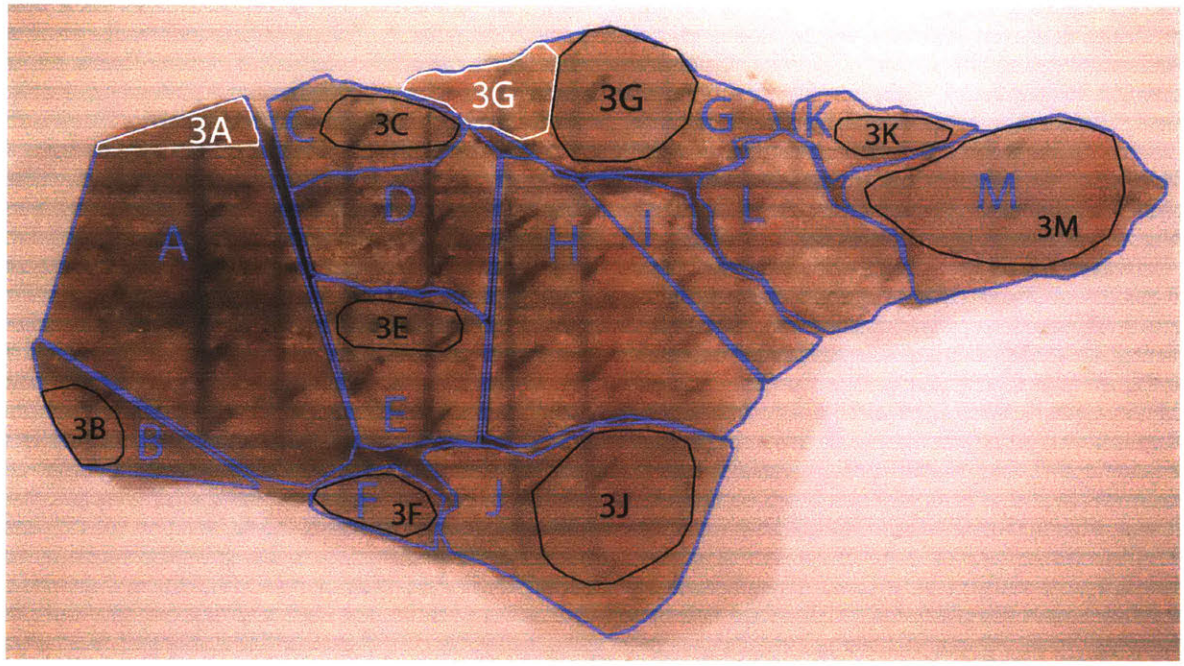

Figure 2-13: Ivysaur Section 3 Guide. Clasts were extracted from 3B, 3C, 3E, 3F, 3G, 3J, 3K, and 3M and are outlined in black. Matrix samples were extracted from 3A and 3G and are outlined in white.

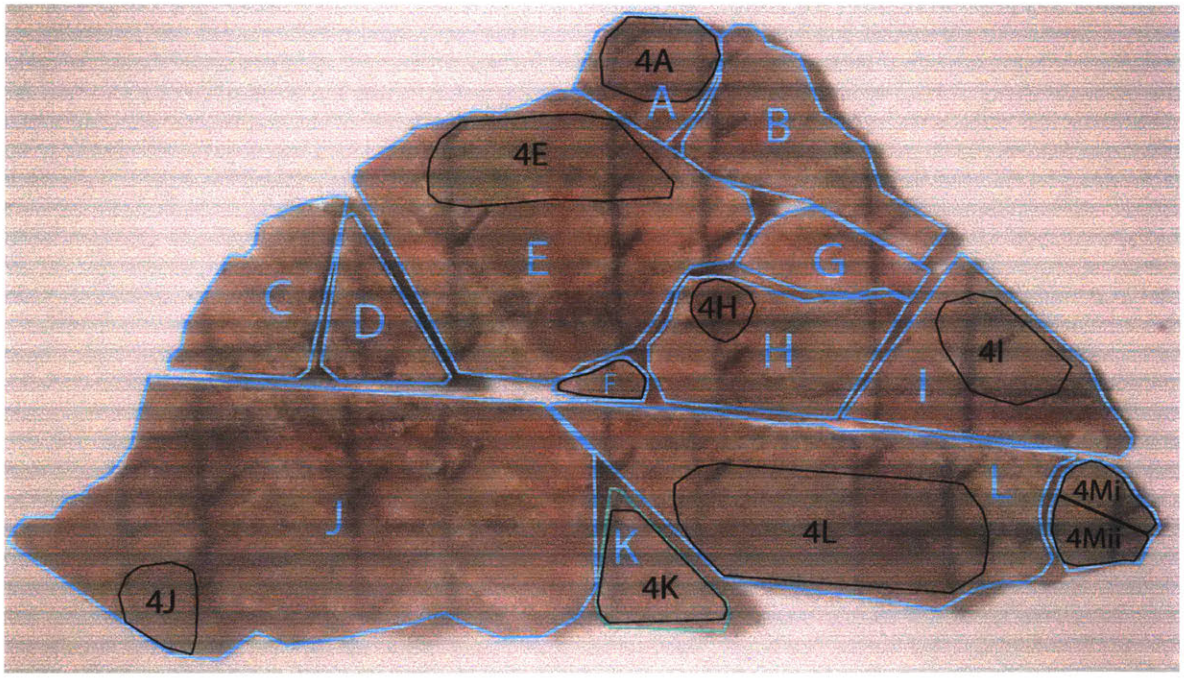

Figure 2-14: Ivysaur Section 4 Guide. Clasts were extracted from 4A, 4E, 4H, 4I, 4J, 4K, 4L, and 4M and are outlined in black. Two clast samples were extracted from 4M which originated from the same parent clast.

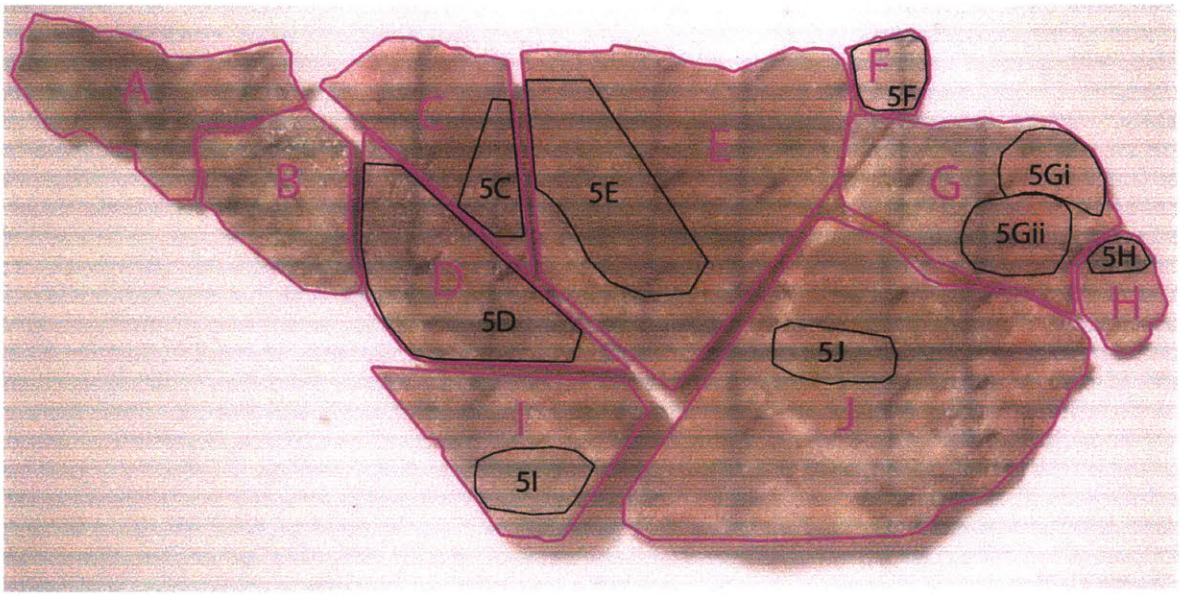

Figure 2-15: Ivysaur Section 5 Guide. Clasts were extracted from 5C, 5D, 5E, 5F, 5G, 5H, 5I and 5 J and are outlined in black. Two clast samples were extracted from 5G which originated from the same parent clast.

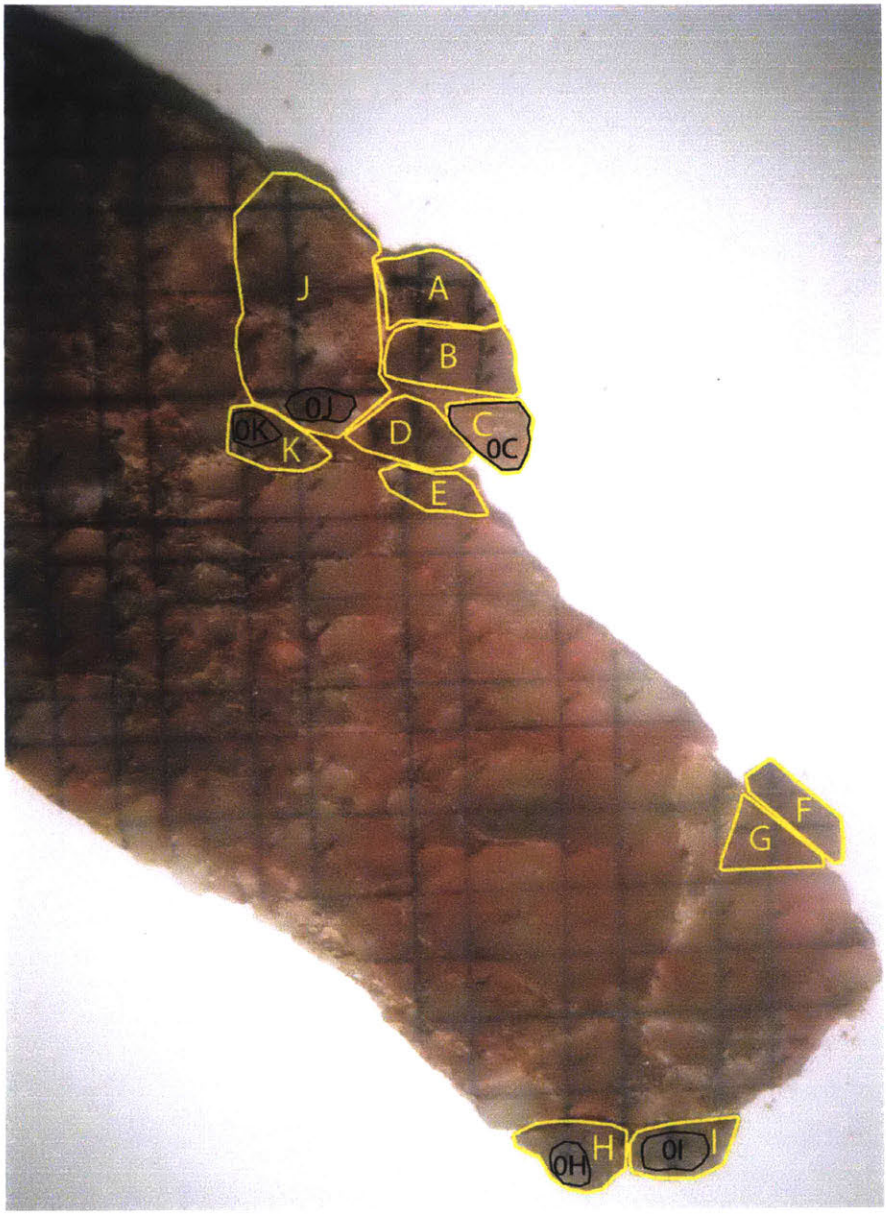

Figure 2-16: Ivysaur Section 0. Pieces which came off while slicing Ivvsaur into a slab have been designated *Ivysaur 0.* Clasts were extracted from 0C, 0H, 0I, 0J and 0K.

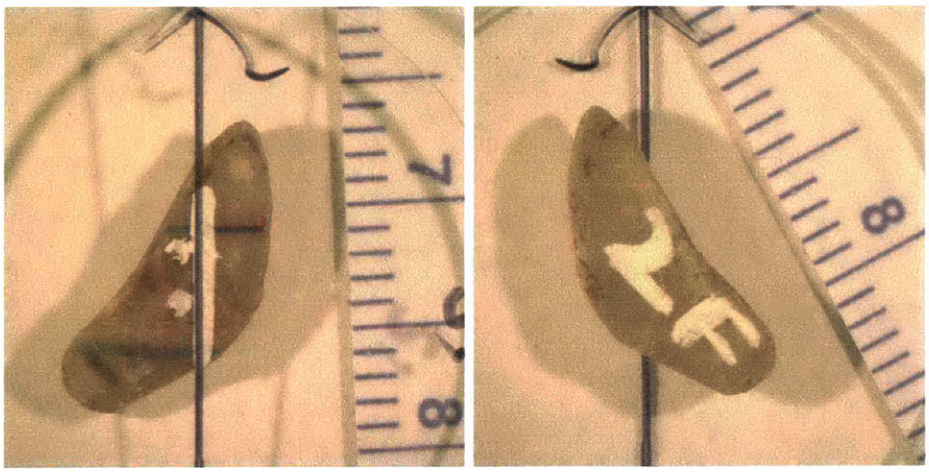

Figure 2-17: Sample 2F on Quartz Disc. Samples were mounted to a quartz disc to be measured using a SQUID magnetometer. A line was drawn on the disc through the sample's "up" direction to help orient the sample in the magnetometer (right hand strike direction is to the right, perpendicular to the drawn line). The ruler in the photos is in centimeters. (left) Harvard side of 2F. (right) Non-Harvard side of 2F. The quartz disc and the Harvard side of 2F are resting flat on the table.

Figure 2-18: Loading Samples in Oven. (Left) To load the samples into the oven, the samples were placed in a glass "boat" which was then slid into the oven. (Right) The samples were loaded unidirectionally. For each temperature step, they were turned to face the alternating direction in/out of the oven.

Chapter 3

Results

Measurements were performed on clasts and matrix samples from the Ivysaur layer which included sections Bulbasaur, Ivysaur 0, and Ivysaur 1 through 5. No samples from the Charmander and Squirtle layers were measured.

Before thermal demagnetization began, the 41 extracted clasts were screened. Eleven clasts (including clast 0C, 2G, 3C, 3E, 4J, 5D, and all clasts from Ivysaur 1) were removed because of matrix contamination. In addition, one clast (0C) was removed because of orientation issues. 29 clasts remained at the start of thermal demagnetization.

From the eight original matrix samples, one sample (s1K) was removed before demagnetization because of an orientation issue. Seven matrix samples remained at the start of thermal demagnetization.

3.1 Demagnetization of Bulbasaur

As a quick trial in preparation for a more detailed demagnetization, the five extracted clasts from the Bulbasaur section were demagnetized using large thermal steps. The samples were heated in 100°C increments, starting at 175°C after measuring the NRM. Figure 3-1 shows an Equal Area Plot and Orthographic Projection of the demagnetization of one of the Bulbasaur clasts. The data suggest that the clasts have a Curie point between 275°C and 375°C.

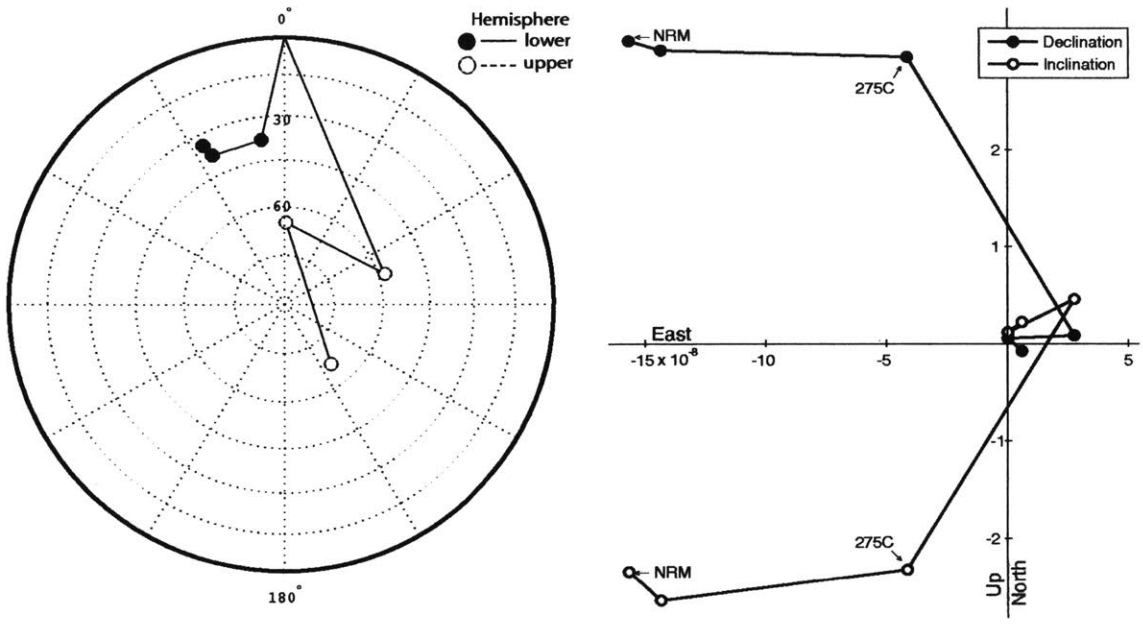

Figure 3-1: Demagnetization of Bulbasaur Clast: Bulb2Gii. Bulb2Gii became demagnetized between 275°C and 375°C. (right) Equal Area Plot of Thermal Demagnetization (left) Orthographic Projection

3.2 Demagnetization of Ivysaur

Guided by the measurements of the clasts in the Bulbasaur section, the Ivysaur clast and matrix samples were heated gradually, with the most detailed inspection between 325°C and 395°C. Matrix samples were heated above 395°C until 650°C. Table 3.1 gives a summary of the complete thermal demagnetization of the Ivysaur samples.

At 200°C, the glue holding the samples on the quartz discs began to weaken. To counter this weakening, a drop of glue was added to each sample as it was removed from the oven. If a sample became unattached from its dish, the dish was cleaned with acetone and the sample was reglued and remarked. At 335°C (and every temperature step higher), the glue did not hold any sample to the quartz disc, so all samples were reglued.

On occasion the white-out orientation marks would fade. When the lines became

Table 3.1: Summary of Thermal Demagnetization Steps

Temp(°C)	Material	# Remounted	# Repainted
NRM	Clast, Matrix	–	–
75	Clast, Matrix	0	0
150	Clast, Matrix	8†	0
200	Clast, Matrix	0	0
250	Clast, Matrix	0	0
275	Clast, Matrix	0	0
300	Clast, Matrix	4†	0
325*	Clast, Matrix	15†	0
335	Clast, Matrix	all	5‡
345	Clast, Matrix	all	0
355	Clast, Matrix	all	0
365	Clast, Matrix	all	0
375	Clast, Matrix	all	2‡
385	Clast, Matrix	all	3‡
395	Clast, Matrix	all	5‡
405	Matrix	all	0
450	Matrix	all	0
500	Matrix	all	0
550	Matrix	all	0
600	Matrix	all	0
650	Matrix	all	0

* Clasts *2AB* and *5J* were removed after being heated to 325°C.
† Remounted samples at temperature 150°C were *0H, 0J, 4A, s1K, s2B, s2Kii, s3A,* and *s3G.* Remounted samples at temperature 300°C were *0I, 3J, 5Gii,* and *s3a.* Remounted samples at temperature 325°C were *0J, 3F, 3J, 3K, 4A, 4F, 4L, 4Mi, 4Mii, 5C, 5F, 5Gi, 5Gii, 5I,* and *s2B.*
‡ Repainted (and remounted after painting) samples at temperature 335°C were *4H, 5F, 5I, s1F, s1H,* and *s2Ki.* Repainted samples at temperature 375°C were *4F* and *s3A.* Repainted samples at temperature 385°C were *0J, 4K,* and *5H.* Repainted samples at temperature 395°C were *2AA, 4F, 4Mii, 5Gii,* and *s2B.*

too difficult to see, the orientation lines would be repainted using pictures of the original lines.

3.2.1 Demagnetization of Clasts

Most clasts displayed two directional components during the demagnetization. One direction was observed in a range between the NRM measurement up to 200°C or 250°C. The second direction was observed from approximately 275°C to 335°C. Table 4.2 lists these clasts, and Figure 3-2 shows an Equal Area Plot and Orthographic Projection of the demagnetization of an of the Ivysaur clasts exhibiting two components.

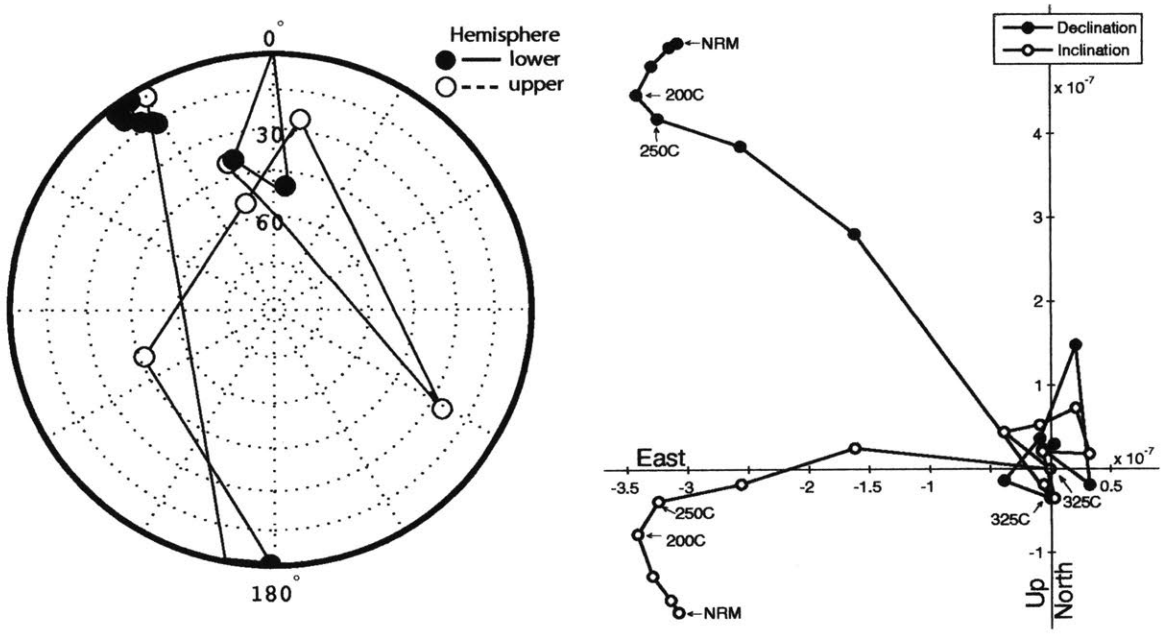

Figure 3-2: Demagnetization of Clast with Two Components: Ivy5H. A low temperature component was observed between NRM and 200°C. The middle temperature component was observed between 250°C and 325°C. (right) Equal Area Plot of Thermal Demagnetization (left) Orthographic Projection

Six clasts displayed only one direction during demagnetization. Table 4.3 lists these clasts, and Figure 3-3 shows an Equal Area Plot and Orthographic Projection of the demagnetization of an of the Ivysaur clasts exhibiting one components.

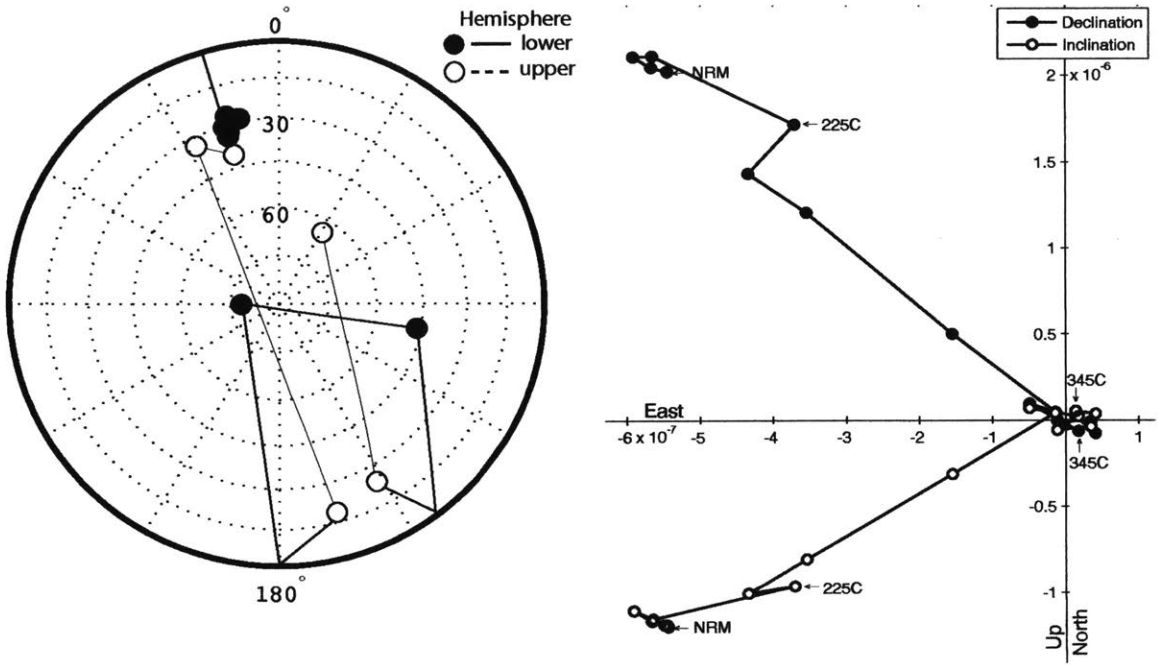

Figure 3-3: Demagnetization of Clast with One Component: Ivy2E. One component was observed between the NRM and 345°C. (right) Equal Area Plot of Thermal Demagnetization (left) Orthographic Projection

Above 355°C, nearly all clasts were completely demagnetized. This can be seen in the plots as scatter that approximately flips magnetization directions every step. This "flipping" is likely due to an overprint from the small magnetic field inside the oven (because each thermal step, the samples were flipped in direction in the oven).

After the temperature step at 325°C, Ivy2AB and Ivy5J were exposed to the Earth's magnetic field. This exposure may have affected the direction of the magnetization, so the two clasts were removed from the rest of the thermal demagnetization.

3.2.2 Demagnetization of Matrix

Thermal Demagnetization of the matrix samples were continued beyond 395°C to 650°C. In general, the matrix samples displayed two clusters of directions. The first cluster included temperatures before the clast demagnetization region (lower than 275°C), while the second cluster occurred after the clast demagnetization region

(higher than 335°C up to 650°C). The matrix samples did not completely demagnetize. Figure 3-4 shows an Equal Area Plot and Orthographic Projection of the demagnetization of one of the matrix samples.

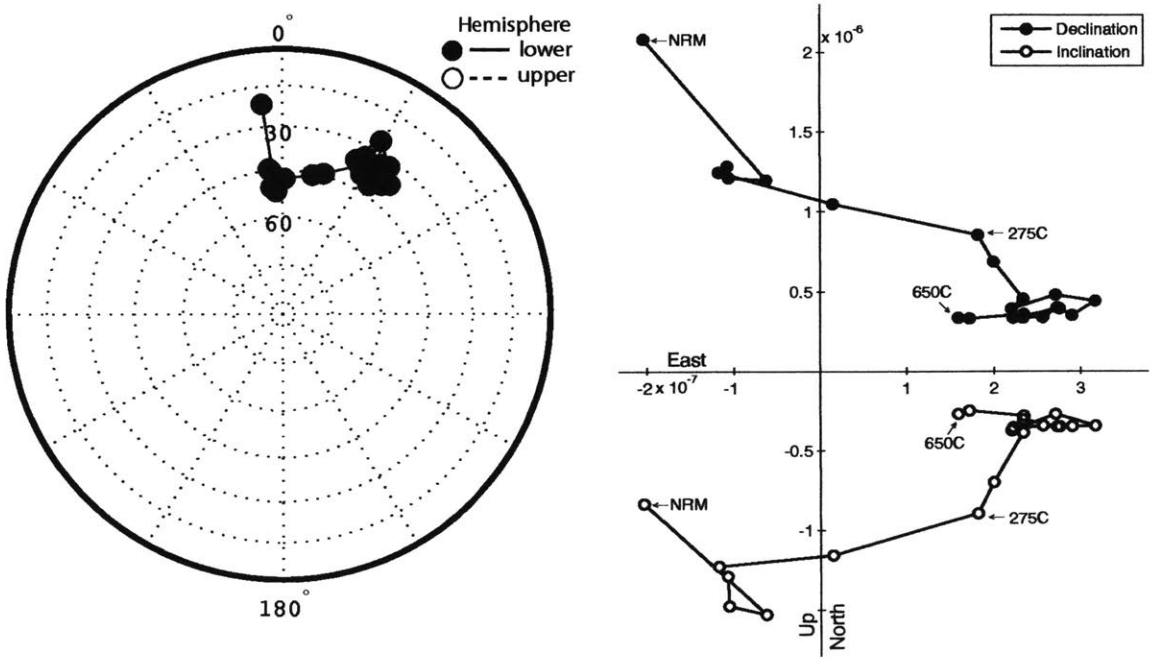

Figure 3-4: Thermal Demagnetization of Matrix: Ivys3A. Two clusters of directions were observed: before the clast demagnetization region (lower than 275°C), and after the clast demagnetization region (higher than 335°C up to 650°C). (right) Equal Area Plot (left) Orthographic Projection

Chapter 4

Analysis

4.1 Finding Average Direction: Least Squares Fit

Least squares fits were made to quantize the direction of the thermal demagnetization within the clast and matrix samples. Equal area plots and orthographic projections were used to determine how many components each sample displayed and what temperature range to perform the fits. The average direction found by the fit was independent of the measured moment of the sample. All least squares fits included at least four temperature points.

The median absolute deviation (MAD) was calculated for each fit and used to screen the data. Least Squares fits with a MAD of over 15 were excluded from further parts of the analysis.

Many clasts showed two components of demagnetization, low temperature (NRM to ~200°C) and middle temperatures (~275°C to ~335°C). (Table 4.1 summaries the low temperature component fits made and Table 4.2 summaries the middle temperature fits made.) The low temperature fits estimated the direction of the overprint, and the middle temperature fit estimated the characteristic magnetization in the clasts. An equal area plot of the fit directions for these components (with MADs) are shown in Figure 4-1 and Figure 4-2 respectively.

Six clasts displayed one unidirectional component and were fit from NRM until the temperature in which the clasts were demagnetized completely (Table 4.3). Clasts

which yielded large MADs at low temperatures were considered for unidirectional fitting. An equal area plot of the fit directions for the unidirectional component (with MADs) is shown in Figure 4-3.

Two directional components of the thermal demagnetization of the matrix samples were fit. The first fits were performed using data in the middle temperature range (same region as the clasts were demagnetized): 275°C to 335°C (Table 4.4). The second component was found using the cluster of high temperature data between 355°C to 600°C. Because the matrix samples did not completely demagnetize, the high temperature fit was forced through the origin to mimic complete demagnetization. This high temperature fit estimated the characteristic magnetization of the minerals in the matrix. An equal area plot of the fit directions for these components (with MADs) are shown in Figure 4-4 and Figure 4-5 respectively.

4.2 Combining Average Directions: Fisher Stats

After least squares fitting was complete, the mean direction (inclination and declination) for each component were found using vector addition. The directions for each of the fits were treated as unit vectors and were then summed to find the declination, inclination, and the length of the resulting mean vector (R). The 95% confidence bound surrounding the average direction (α_{95}) was also determined.

Samples were then analyzed using Fisher Statistics, a common method of analysis used in paleomagnetism. The spread of the data are represented in the Fisher probability density function:

$$P_{dA}(\theta) = \frac{\kappa}{4\pi \sinh(\kappa)} \exp(\kappa \cos\theta) \tag{4.1}$$

where $P_dA(\alpha)$ is the probability per angular area of finding a point within an area, θ is angle between the mean vector and the true direction, and κ is the dispersion factor (Fisher 1953 and Tauxe 2010). The more spread the direction measurement, the smaller the value for κ will be. Table 4.6 gives a summary of the analysis to find the mean direction and Fisher statistics for the low, mid, and one component

Table 4.1: Least Squares Fit Clasts - Low Temperature

Sample	Range ↓	Range ↑(°C)	dec (°)	inc (°)	N	MAD
IVY0H	NRM	200	74.8	-83.2	4	8.8
IVY0I	NRM	200	81.8	-70.4	4	28.6
IVY0J	NRM	200	39	-32.2	4	9.1
IVY0K	NRM	250	152.1	46.6	8	19.7
IVY2AA	NRM	200	119.4	-19	4	38.1
IVY2AB	NRM	200	143.4	76	4	26.3
IVY2C	NRM	200	64.9	70.2	4	19
IVY2F	NRM	250	35.9	-38.2	5	13.7
IVY2J	NRM	250	328.4	-14.3	5	13.6
IVY2L	NRM	200	129.9	-6.4	4	10.7
IVY3F	NRM	200	330.6	18.2	4	4.5
IVY3G	NRM	200	331.7	-21.2	4	20
IVY3J	NRM	250	7.8	-8.3	5	11.2
IVY3K	NRM	250	340.9	-11.3	5	10.4
IVY4A	NRM	200	23.1	-26.4	4	13.3
IVY4E	NRM	150	334	-15.1	3	1.8
IVY4F	NRM	200	164.1	62	4	13
IVY4H	NRM	200	336.9	-34.4	4	4.3
IVY4K	NRM	200	137.8	76.2	4	37.5
IVY4L	NRM	200	323.9	59.6	4	24.6
IVY4Mii	NRM	200	297.6	16.4	4	1.4
IVY5C	NRM	200	325.7	-7.2	4	8.2
IVY5E	NRM	200	85.1	-23.4	4	27
IVY5F	NRM	200	342.1	-56.5	4	2.4
IVY5Gi	NRM	200	318.1	54.7	4	16.4
IVY5Gii	NRM	200	134.8	-1.1	4	21
IVY5H	NRM	200	27.9	52.4	4	3.6
IVY5I	NRM	200	242.9	-46.1	4	8.1

Table 4.2: Least Squares Fit Clasts - Middle Temperature Region

Sample	Range ↓ (°C)	Range ↑ (°C)	dec (°)	inc (°)	N	MAD
IVY0H	275	335	330	2.9	4	19.3
IVY0I	275	335	338.5	18	4	6.7
IVY0J	275	335	334.6	7.3	4	6.4
IVY0K	250	335	343.1	-49.3	5	9.3
IVY2AA	250	335	319.4	-5.2	5	3.7
IVY2C	275	335	340	3.1	4	6.3
IVY2E	275	335	343.3	35.5	4	1
IVY2F	275	335	355.9	39.7	4	4.6
IVY2J	275	335	263.6	76.6	4	2.7
IVY2L	250	335	332.2	-3.1	5	15.3
IVY3G	275	345	334.1	12.5	5	10.5
IVY3J	275	345	325.1	8.2	5	12.1
IVY3K	275	335	321.7	49.4	4	9.6
IVY3M	275	335	343.4	26.3	4	6.2
IVY4A	275	345	325.7	38.6	5	15.2
IVY4E	275	345	333.8	3.7	5	9.8
IVY4F	250	345	331.3	23.7	6	7
IVY4H	275	335	319.4	9.5	4	5
IVY4I	275	335	298	-2.8	4	13.2
IVY4K	275	335	325.3	1.8	4	2
IVY4L	275	335	329.6	-4.6	4	1.7
IVY5C	275	335	331.7	18.6	4	4.2
IVY5E	275	335	336.2	13.1	4	2.5
IVY5F	275	335	40.8	41.2	4	13.3
IVY5Gi	275	335	319.2	-31.5	4	11.8
IVY5Gii	275	335	321.7	26.8	4	8.7
IVY5H	250	325	326.1	3.2	4	7.9
IVY5I	275	335	343.3	-11.1	4	8.5

Table 4.3: Least Squares Fit Clasts - One Component

Sample	Range ↓ (°C)	Range ↑ (°C)	dec (°)	inc (°)	N	MAD
IVY2E	NRM	345	345.3	30	10	5.1
IVY3F	NRM	395	333.2	29.3	15	9.4
IVY3M	NRM	345	343.8	24.7	10	4.6
IVY4E	NRM	345	332.9	7.2	10	5.7
IVY4K	NRM	335	326.7	4.5	9	4
IVY4L	NRM	335	330.7	-6.4	9	2.8

Table 4.4: Least Squares Fit Matrix - Middle Temperature Region

Sample	Range ↓ (°C)	Range ↑ (°C)	dec (°)	inc (°)	N	MAD
IVYs1F	275	335	19.9	3.2	4	0.8
IVYs1H	275	335	354.4	8.9	4	3.8
IVYs2B	275	335	359.3	0.4	4	4.6
IVYs2Ki	275	335	3.7	20.5	4	7.7
IVYs2Kii	275	335	19.4	29.4	4	7.3
IVYs3A	275	335	340.8	50.5	4	6.1
IVYs3G	275	335	360	26.1	4	9

Table 4.5: Least Squares Fit Matrix - High Temperature Region

Sample	Range ↓ (°C)	Range ↑ (°C)	dec (°)	inc (°)	N	MAD
IVYs1F	355	600	11.8	-26.5	10	12.2
IVYs1H	355	600	38.5	0.9	10	2.5
IVYs2B	355	600	0.1	-19.3	10	9.3
IVYs2Ki	355	600	37.7	8	10	6.8
IVYs2Kii	355	600	37.9	6.3	10	6.4
IVYs3A	355	600	34.2	35.1	10	4.9
IVYs3G	355	600	325.6	-29.9	10	28.7

temperature range fits for the clasts and the mid and high range fits for the matrix. Fisher Statistics calculations were completed using the software *PaleoMag v 3.1d39.*

Figure 4-6 shows an Equal Area plot with the results of the Fisher Analysis for the low and middle temperature clast components and the middle and high temperature matrix components. (The unidirectional clasts were excluded from this plot, because they were redundant with the middle temperature clasts.) The four components resided in the North direction and had a low inclination. The low temperature clast component overlapped in direction with the mid temperature clast and matrix components, although the direction had a large uncertainty (α_{95}=36.02°). This unexpectedly largely dispersion in comparison to the middle temperature components ($\kappa_{low} = 1.97 < \kappa_{mid}$=7.30) indicates that this overprint is not simply explained by viscous remanent magnetization from exposure to the Earth's present field.

A Watson (1956) test was then performed to determine if each set of data was random (Watson 1956). The Watson parameter (R_0), which was determined by the

Table 4.6: Summary of Fisher Statistics Results

	Comp	dec(°)	inc(°)	α_{95}(°)	κ	N_{fit}	N_{tot}	R	R_0*
Clast	L	345.8	-20.3	36.02	1.97	16	29	8.4	6.4
Clast	P	332.1	13.1	11.51	7.30	25	27	21.7	8.07
Clast	one	335.1	15	14.09	19.65	6	6	5.8	3.85
Matrix	P	3.4	20.1	16.28	12.59	7	7	6.6	4.18
Matrix	H	27.1	0.7	23.57	7.53	6	7	5.4	3.85

* The Watson parameters were found by referencing Table C.2 in Tauxe 2010. R_0 refers to 95% confidence.

number of points (N_{fit}) used to fit for each component, was compared to the length of resulting mean vector (R). If the length of the resulting mean vector $R < R_0$, the set of data was considered random (Tauxe 2011). For the low and high temperature components of the clasts and matrix, the Watson parameter was larger than the resulting mean vector ($R_0 < R$), indicating no set was random to the 95% confidence interval.

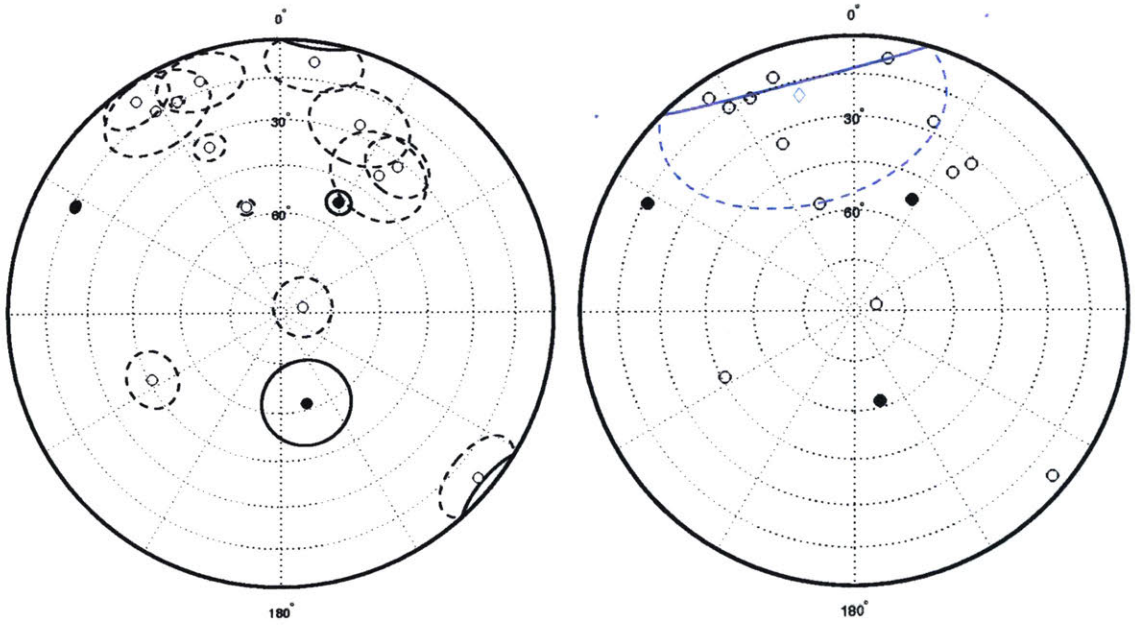

Figure 4-1: Equal Area Plot of Clasts for Low Temperature. (Left) The declination and inclination produced from the low temperature least squares fits are plotted with their MAD. (Right) The declination and inclination produced from the low temperature least squares fits are plotted with their average value and 95% confidence boundary. The average direction is represented by a blue diamond.

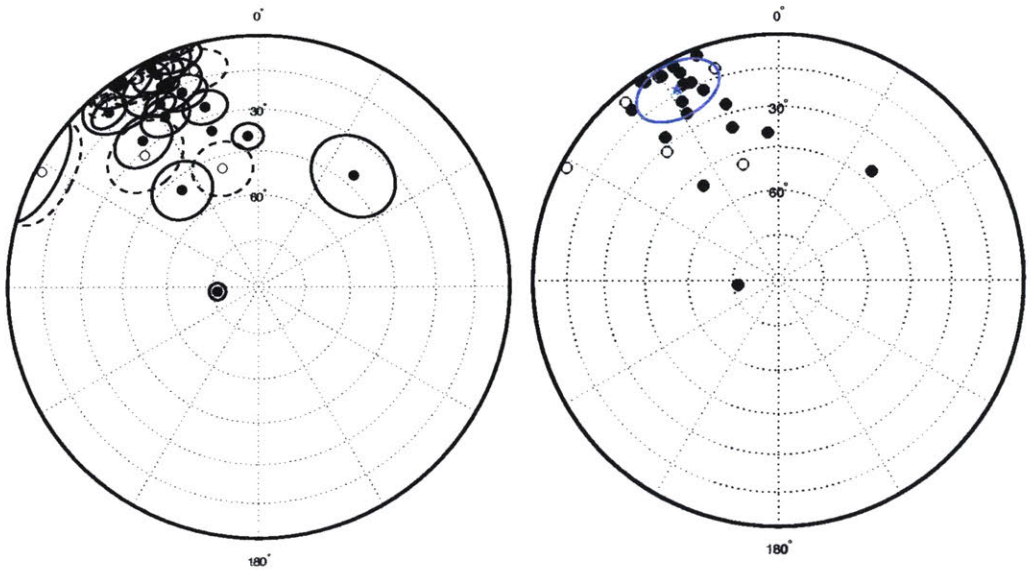

Figure 4-2: Equal Area Plot of Clasts for Mid Temperature. (Left) The declination and inclination produced from the mid temperature least squares fits are plotted with their MAD. (Right) The declination and inclination produced from the pyrrhotite region least squares fits are plotted with their average value and 95% confidence boundary. The average direction is represented by a blue star.

4.3 Unaccounted for Error Sources

Several sources of random and systematic error have not been accounted for in the analysis described in sections 4.1 and 4.2. If these errors were included in the analysis, the estimate for the uncertainty for each measurement would increase. This would propagate to also increase the 95% confidence bound estimate (α_{95}) on each of the average directions obtained using Fisher statistics.

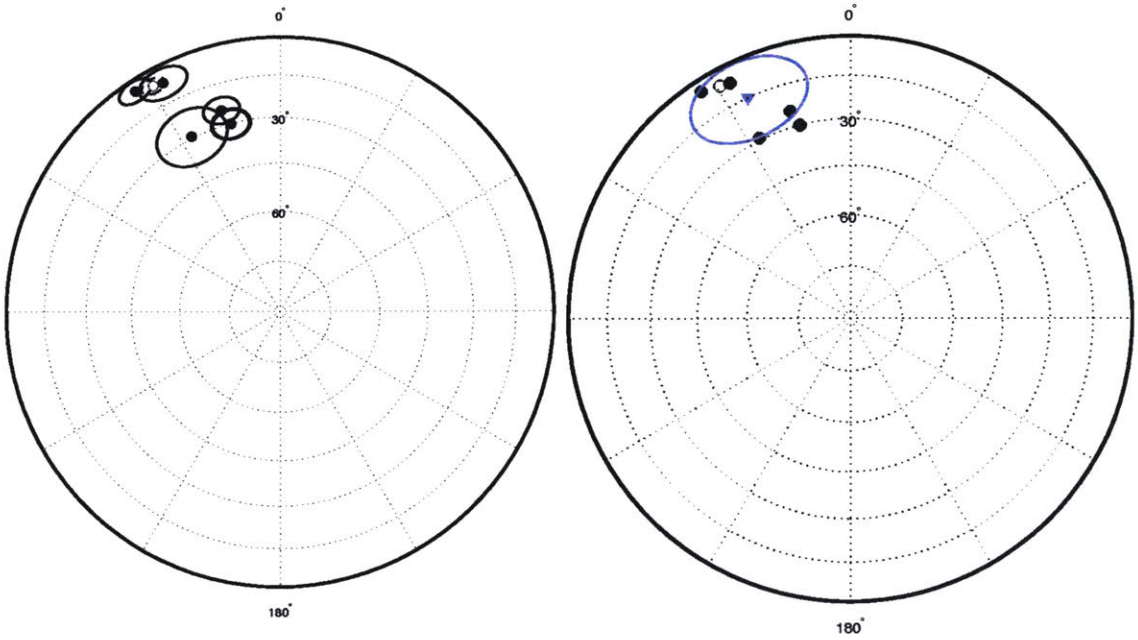

Figure 4-3: Equal Area Plot of Clasts Displaying One Component. Clasts with one unidirectional component were pointing in a similar direction to each other and to the mid temperature clast component. (Left) The declination and inclination produced from the least squares fits are plotted with their MAD. (Right) The declination and inclination produced from the low temperature least squares fits are plotted with their average value and 95% confidence boundary. The average direction is represented by a blue triangle.

4.3.1 Unaccounted for Random Error

For every measurement, the sample needed to be aligned by hand on the magnetometer. The orientation of the sample's declination was not constrained during this alignment. Small deviations in the declination of approximately 3° occurred.

After high temperature thermal steps, the samples were reglued and the orientation line was redrawn. Small changes were made in the redrawing of orientation lines on the quartz discs which also caused small deviations in the declination of approximately 3°. This could have been corrected by photographing each step and applying a correction by comparing photos.

Small amounts of crumbling were observed when samples were transported (especially for the matrix samples). The amount of crumbling was not quantified, and could have affected the overall moment of the sample.

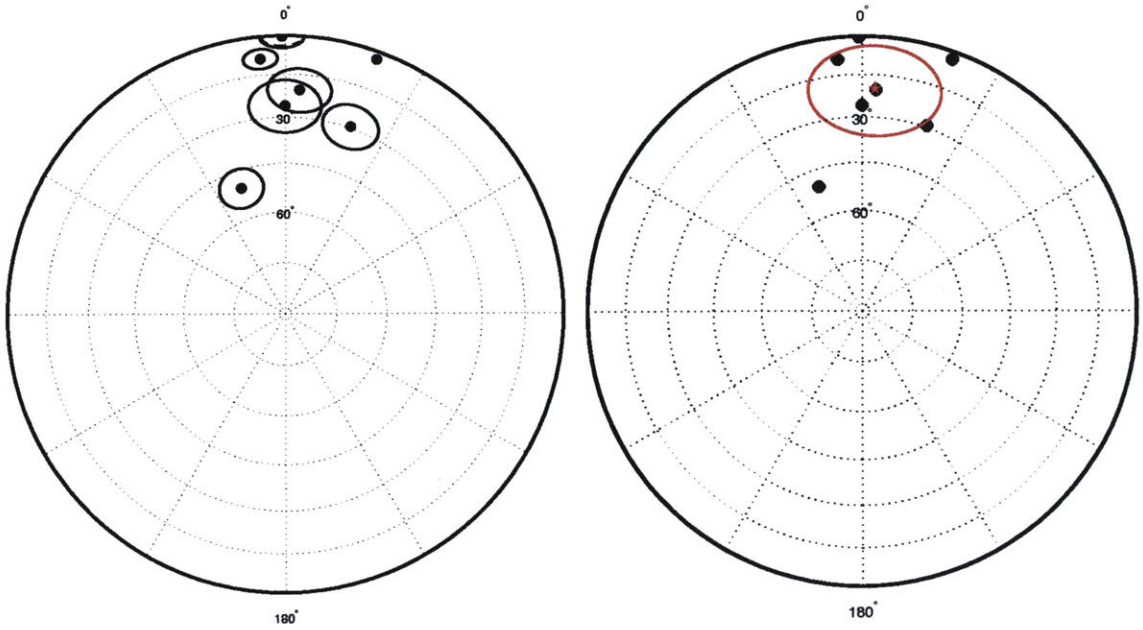

Figure 4-4: Equal Area Plot of Matrix for Mid Temperature. (Left) The declination and inclination produced from the mid temperature least squares fits are plotted with their MAD. (Right) The declination and inclination produced from the pyrrhotite region least squares fits are plotted with their average value and 95% confidence boundary. The average direction is represented by a red star.

4.3.2 Unaccounted for Systematic Error

Occasionally the orientation line on a sample would fade and the sample would have to be remarked and/or repainted with white out. This may have caused a shift in the declination for measurements. Pictures taken before and after the remarking could be used to help correct for any declination offset caused by the remarking.

Although clasts with significant matrix material on them were removed from the thermal demagnetization process, some clasts still contained minimal amounts of matrix. At high temperatures, the matrix remaining on the samples contributed more significantly to the direction, trending the clast to be in the same direction as the matrix. This could be checked by reviewing the amount and placement of any matrix material that is left on the clasts.

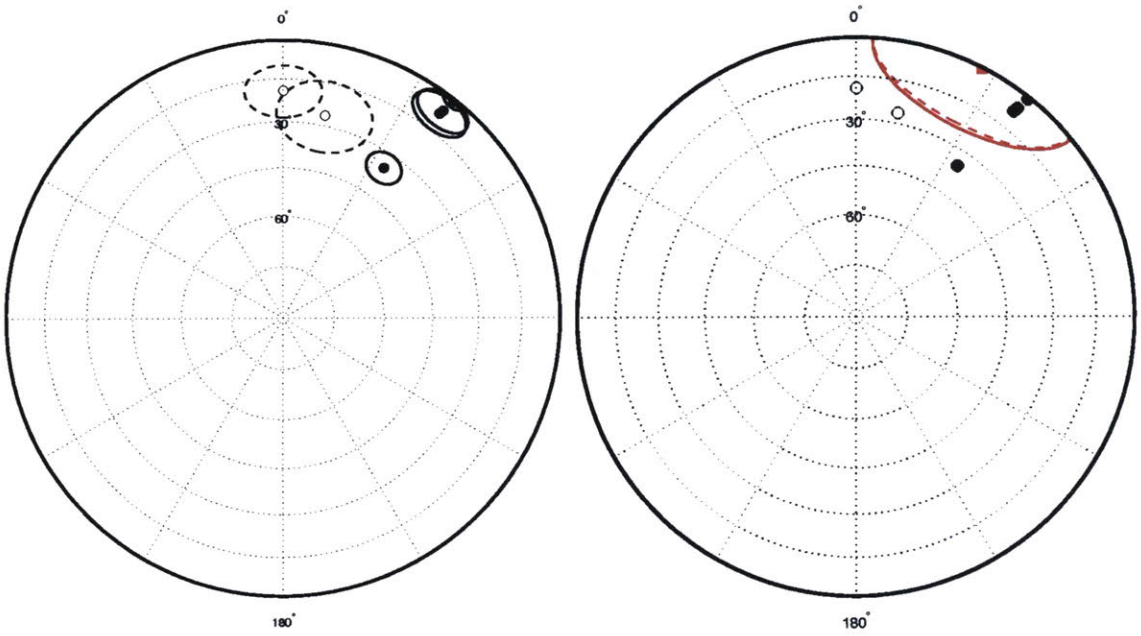

Figure 4-5: Equal Area Plot of Matrix for High Temperature. A cluster of high temperature points for each matrix sample were fit forced through the origin (to simulate complete demagnetization of the matrix). (Left) The declination and inclination produced from the high temperature region least squares fits are plotted with their MAD. (Right) The declination and inclination produced from the pyrrhotite region least squares fits are plotted with their average value and 95% confidence boundary. The average direction is represented by a red square.

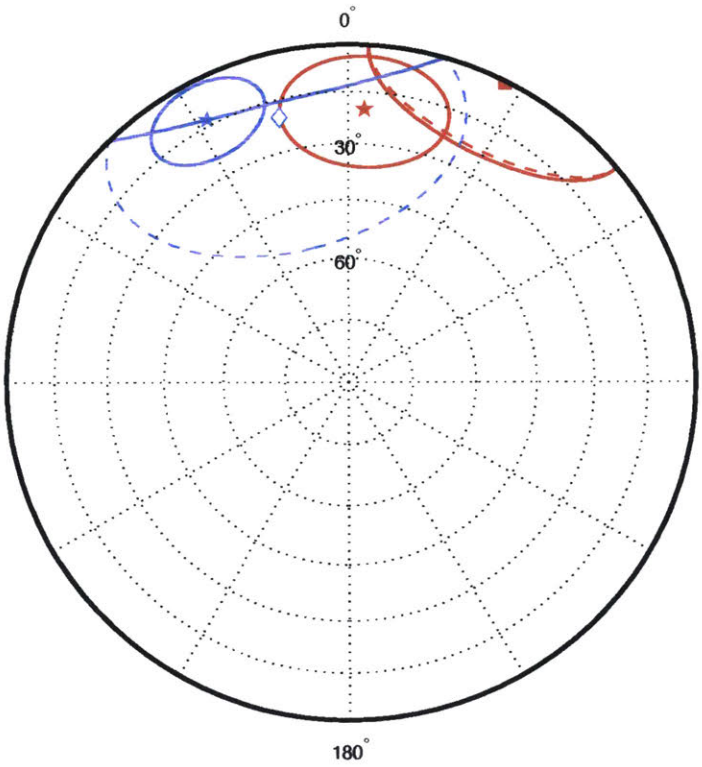

Figure 4-6: Overall Magnetization of Ivysaur. The points and lines in blue represent the clast while the red represents the matrix. The diamond is the low temperature component, the star is the mid temperature region and the square is the high temperature component. The direction of the four components are in the same region of the equal area plot. (The unidirectional clast component is not shown.)

Chapter 5

Conclusion

5.1 Mineralogy

The measured demagnetization in the clasts was characteristic of the mineral Pyrrhotite (Fe_7S_8). Pyrrhotite is known to have a Currie point of 325°C, which varies slightly depending on grain size (Dekkers, 1989). This matched the observed demagnetization range of approximately 275°C to 335°C.

The measured demagnetization in matrix material was characteristic of the mineral Hematite (αFe_2O_3). The matrix material was heated to 650°C and was not demagnetized. The two magnetic minerals with the highest demagnetization temperatures are Magnetite (T_{currie}=580°C) and Hematite (T_{neel}=675°C) (Tauxe, 2010). Because the samples were not demagnetized, the data supports that the magnetic carrier in the matrix was Hematite.

5.2 Conglomerate test

The clasts measured from the Ivysaur section of EHJH5 failed the conglomerate test. The data around the demagnetization of Pyrrhotite was fit for each clast to reveal the direction of the characteristic magnetization. These fits were then analyzed using Fisher statistics, and a Watson's test of randomness was performed. The average mean vector resulting for the Pyrrhotite demagnetization ($R = 21.7$) was larger than

the Watson parameter corresponding to that the data set (R_0=8.07) (Tauxe, 2010). Therefore, the clast directions were not random to a 95% certainty.

The direction of the characteristic magnetization in the clasts were also similar to the low temperature overprint in the clasts as well as the mid and high temperature components of the matrix samples. This similarity in direction further supports that the sample was remagnetized after its formation.

5.3 Future Work

In order to meet the original goal of measuring the oldest recorded magnetic record, a new sample must be studied. Another conglomerate rock would need to be tested from the Jack Hills area or another place on Earth containing ancient crust.

Appendix A

Recommendations for Future Work

A.1 Use High Temperature Glue

Using a high temperature, non-magnetic glue would not only reduce the time it took to complete each thermal step but would also the orientation of the samples more consistent reducing random error in the declination. The most non-magnetic high temperature glue known by the Paleomagnetism Lab at MIT is *SPI Silver Paste Plus*. One disadvantage to this glue is that it does not dry clear, so orientation marks made on the rocks cannot be seen. It has also not been tested during alternating field and other demagnetizations.

A.2 Strategically Use Small Temperature Steps

Thinking ahead about the properties about the magnetic carrying mineral in the sample would yield a more complete set of data. For rocks which may are known to commonly contain minerals with a low currie point (like pyrrhotite in Archean rocks), use smaller step sizes early in the demagnetization. Using smaller step sizes between 275° and 335° would have made the demagnetization direction in each sample more clear.

A.3 Expect to Lose Samples

Expect a number of samples to not make it through the demagnetization process. When performing a conglomerate test, it is important to gather data from samples from the same parent clast. Make sure to sub-sample enough parent clasts where if some are lost, a consistency check can still be completed. Do not choose small parent clasts. Use larger samples so the sub-samples will have a strong magnetic moment and not be lost to noise.

A.4 Mark Samples Simply

Use different colors for orientation lines in perpendicular directions (for example chose black for the up-down lines and red for the lines in the direction of the strike). Different colored lines will make orienting smaller pieces more obvious. Thin sharpie should be used to draw these line, and markings like arrows should be drawn with the standard convention(pointing in the strike direction).

A.5 Use Pokemon as part of the naming convention for samples.

Naming sections of rock after Pokemon avoided confusion and allowed for quick recognition of rock pieces. A problem which arose while trying to determine a naming convention for the slabs is that numbers, letters, and roman numerals were already being used to name pieces and clasts/matrix. By using Pokemon names, doubling was avoided.

When one of the layers (Ivysaur/Bulbasaur) had a special section (Bulbasaur), the section could be easily designated as "special" (because it didn't share the Ivy prefix). Yet the section still shared an association with the rest of the layer (because it was within the same evolutionary family), so it was easy to remember that they were a part of the same layer. It was also easy to remember that Bulbasaur refereed

to the section piece (because the Pokemon Bulbasaur is smaller than Ivysaur).

In addition, Charmander, Squirtle, and Bulbasaur/Ivysaur have pre-associated colors. The slabs and containers holding the pieces cut from these slabs were marked in the correct color allowing rocks to be matched with others on the same layer at a quick glance.

Bibliography

[1] Biggin, A. et al., 2011. *Palaeomagnetism of Archaean rocks of the Onverwacht Group, Barberton Greenstone Belt (southern Africa): Evidence for a stable and potentially reversing geomagnetic field at ca. 3.5 Ga*, Earth and Planetary Science Letters, 302, Pages 314-328

[2] Butler, R.F., 1992. *Paleomagnetism*, Cambridge, MA: Blackwell Scientific Publications.

[3] Buz, Jennifer. *Lunar Magnetism in the Last 9000 Years.* Undergraduate Thesis. Massachusetts Institute of Technology, Cambridge, 2010.

[4] Dekkers, M.J., 1989. *Magnetic Properties of Natural Pyrrhotite. II. High- and Low-Temperature Behaviour of Jrs and TRM as Function of Grain Size*, Physics of The Earth and Planetary Interiors, 57: 266 - 283.

[5] Fisher, R.A., 1953. Dispersion on a sphere. *Proceedings of the Royal Society of London*, Series A, 217: 295305.

[6] Kirschvink, J. L.,1980. *The Least Squares Line and Plane and the Analysis of Paleomagnetic Data*, Geophysical Journal. Royal Astronomical Society, 62, 699-718.

[7] Spaggiari, C. et al., 2007. *The Jack Hills greenstone belt, Western Australia Part 2 Lithological relationships and implications for the deposition of detrital zircons*, Precambrian Research 155.

[8] Spaggiari, C. et al., 2008. *Proterozoic Deformation in the Northwest of the Archean Yilgarn, West Australia*, Precambrian Research 162, 354-384.

[9] Tarduno, J., et al., 2010. *Geodynamo, Solar Wind, and Magnetopause 3.4 to 3.45 Billion Years Ago*, Science 327, 1238.

[10] Tauxe, L., *Essentials of Paleomagnetism*, University of California Press, 2010.

[11] Usui, Y. et al., 2009. *Evidence for a 3.45-billion-year-old Magnetic Remanence: Hints of an Ancient Geodynamo from Conglomerates of South Africa*, Geochemistry Geophysic Geosystems, Volume 10, Number 9, 1525-2027.

[12] Watson, G. S., 1956. *Analysis of dispersion on a sphere*, Mon. Not. Roy. Astr. Soc, Geophys. Suppl. 7, 153159.

[13] Watson, G. S. & Irving, E., 1957. *Statistical methods in rock magnetism*, Mon. Not. Roy. Astr. Soc, Geophys. Suppl. 7, 289300.